Report on a problem studied at the UK Mathematics-in-Medicine Study Group Keele 2012
< https://mmsg.mathmos.net/uk/2012/magnetic-stem-cells/ >

Targeting stem cells following I.V. injection using magnetic particle based approaches

M. Albert-Gimeno, I. Hadji, T. Joshi, L. Kimpton, T. Kwan, G. Lang, S. Moise, S. Naire, F. Nouri, G. Richardson, R. Whittaker

December 6, 2012

Abstract

Magnetic labelling has been suggested as a way to guide mesenchymal stem cells out of the bloodstream, at a target site in the body for therapeutic use. Here we consider the magnetic forces involved and how they compete with the forces on a cell caused by blood flow in a number of different situations.

1 Introduction

Characterised by the ability of self-renewal and multipotency [26], stem cells have been put under both the literal and metaphorical microscope and are now seated as the potential 'cure' for innumerable diseases. Whilst the potential of embryonic stem cells is further reaching due to their vast differentiation capacity; mesenchymal stem cells (MSCs) hold promise, especially within the field of orthopaedics, with their characteristic trilineage in vitro differentiation into osteoblasts, chondrocytes and adipocytes [5]. First isolated from bone marrow [23], MSCs are now known to reside in a multitude of tissues including adipose, amniotic fluid, placenta, and umbilical cord vein [13, 28, 29, 33], making them an attractively accessible option in cellular therapies.

Alongside the in vitro culture and 'creation' of implantable tissues, MSCs have been harnessed in tissue repair through their modulatory activities [20], such as that on the innate and adaptive immune systems. Such regulatory effects contribute to the in vivo demonstrated clinical efficacy of MSCs in an abundance of diseases and disease processes including myocardial infarction, rheumatoid arthritis, retinal degeneration, acute lung injury, and hepatic failure [31].

The majority of orthopaedics tissues have become targets for cellular therapies, with the repair of cartilage defects, tendons, and intervertebral discs high on the agenda [3]. Usually such therapies introduce cells through local delivery i.e. direct injection or surgical implantation; however this method is not without its limitations. Inaccessible locations, multiple sites, the need for repeated dosages and non-surgical candidates, all highlight the requirement for the need of a minimally-invasive systemic means of delivering MSCs to their intended site(s) of action.

Ample literature already exists on the systemic delivery of MSCs including that on safety, their natural 'homing' capabilities, and the targeting of specific organs or tissues.

The innate ability of MSCs to 'home' in on an area of tissue injury lies in similarities to leukocyte migration, with many of the leukocyte chemokine receptors also expressed on MSCs [4]. For migration across endothelium to occur, MSCs must first become adherent to the endothelial surface in a process characterised in leukocytes [18]. Extravasation of leukocytes first starts with the rolling of the cell along the endothelial surface. Interaction of various cell-surface receptors with their ligands initiates activation and slow rolling of the cell before arrest occurs. Adhesion occurs as a result of inflammatory cytokines from the insulted tissue stimulating endothelial cells lining blood vessels to express adhesion molecules following which the cell begins to crawl along the vessel lumen in response to integrins (MAC1, ICAM1) in search of preferred sites of transmigration, which occurs paracellularly or transcellularly. The inhibition of crawling has been shown to delay transmigration and give preference to the transcellular pathway. MSCs have been shown to exhibit rolling and adhesion along endothelial surfaces, which is reduced in P-selectin deficient mice [27].

Currently efforts are being made to improve the homing and migration capacity of MSCs through manipulation of expressed surface receptors via culture conditions (hypoxia; 'cytokine cocktails'; degree of confluency; genetic enhancement) and manipulation of the target site (co-administration with aspirin, heparin, or regulatory T cells; electrical stimulation of site) [12]. Whilst the demonstration of relevant adhesion and migration factors on MSCs is encouraging, we are still a long way off utilising this to create an effective and efficient clinical therapy. There is a need to develop an alternate means of inducing a chemotactic-like migration when in vivo conditions will not facilitate natural chemotaxis, i.e. in sub-chronic or chronic disease conditions and a means of enhancing natural MSC migration without alterations in the cell surface receptors or adaptation of the target tissue.

One potential option for this lies in magnetic nanoparticles which have been used previously for therapeutic delivery of drugs to specific sites in the body [30]. The particles consist of a magnetic core, usually iron oxide, in the nanometre scale (the majority: 10-20nm) which is then coated with various polymers to both prevent oxidisation and to also functionalise the particles i.e. with various ligands [19]. The magnetic cores display super-paramagnetic properties (hence their alternate name - Super Paramagnetic Iron Oxide particles [SPIOs]) whereby they are strongly magnetic under the influence of a magnetic field while show no magnetic response when the field is removed. They can therefore be manipulated via an external magnetic field (and human tissue is highly permeable to magnetic fields) with very little residual magnetism remaining when the field is removed, making them ideal for biomedical applications [19, 22].

SPIOs have also been implicated as a potential cancer treatment via induction of hyperthermia to the site through the application of an alternating magnetic field, whilst sparing surrounding tissue. Efficacy has been demonstrated in animal studies but little has been achieved yet in humans. But within humans SPIOs are already clinically in use as MRI contrast agents, with several already FDA approved [22, 16, 11]. Recent research focuses on trapping SPIO-labelled stem cells at target sites using an external magnetic field. Kyrtatos et al, were able to increase the number of endothelial progenitor cells localised to a common carotid artery injury in rats using SPIOs and an externally applied magnetic field [15]. El Haj et al demonstrated increased trapping of MSCs labelled with SPIOs within a subcutaneous wound murine model containing an implanted magnet

[6]. Whilst successful trapping was achieved in both the above studies, they relied on either a superficial target, or an implanted magnet. For further clinical applications, cell targeting will be required at greater depths within the body, and as minimally invasive as possible.

Huang et al [10] produced a magnetic field 'focussed' at a point distant from the magnet surface with a unique arrangement of electromagnets. This method however requires equipment on a large scale and will therefore have limited clinical applicability. Riegler et al [25], studied the use of magnetic resonance imaging equipment to 'guide' cells through a vascular bifurcation phantom, and found that 75% of cells could be guided in this way, promoting that such a method may indeed be clinically feasible. MRI equipment is however expensive to operate and would once again reduce the clinical applicability of such a technique when compared to the use of simple external magnets.

1.1 Questions to address

The primary question put to the study group was to consider whether loading MSCs with magnetic particles would enable them to be directed to specific sites, deep in the tissue with the external application of magnets. Fundamental to this is understanding how the forces due to the bloodflow and the magnetic field compete and control the cell motion in different vessels. If the approach is feasible then there are secondary questions concerning: the optimal number of SPIOs in a cell; predicting the proportion of SPIO-loaded cells that reach the target site; how long MSCs take to reach the target site and for what length of time external magnets should be used.

2 Literature review

The report [24] from the Study Group held in 2000, summarizes some work on a similar problem. The report discusses the physical aspects of the problem, specifically the force experienced by the particles in a vessel due to fluid flow and the externally applied magnetic field. A model was formulated for the motion of a single particle in the blood flow. It was assumed that the vessel is cylindrical with arbitrary cross section and axis lying parallel to x-axis and that the blood flow is Poiseuille, such that all flow is solely in the x-direction and the flow speed depends only on y and z. Initially, motion of a single particle in the blood flow was modelled. Later, the case when the particle due to its motion comes very close to the vessel wall was also modelled. Then a two-dimensional reduction of the model was considered. In this case, the blood vessel was thought of as a channel between two parallel plates separated by a fixed distance and with normals along the y-axis. Phase trajectories of particles moving past the magnets were plotted in the limit where the distance between plates (vessel thickness) is small compared to the distance from the vessel to the magnet. It was observed that reducing the separation between the magnet and the channel increased the number of particles reaching the bottom surface of the channel. Equilibrium positions, denoted as $\hat{x}$, of the particles on the lower boundary of the channel were also obtained. According to the report, the equilibrium which occurs at highest value of $\hat{x}$ is unstable and any particle which reaches the bottom surface before this equilibrium is trapped while the particle which reaches the bottom after the equilibrium is not trapped. It is also suggested that by tracing

the phase trajectories of the particles, an estimate of percentage capture of particles can be obtained. The report suggests some directions for future work including considering the diffusive effects caused by thermal excitations, or determining whether particles that reach the vessel wall are embedded in the sides of the blood vessels so that they remain at the site of injury even after the removal of the magnetic field. Some work was also done to study the effect particle interactions.

Further work on this problem was done and published by Grief and Richardson [8]. An advection-diffusion model is proposed for motion of magnetic particles in the bloodstream. Along with the hydrodynamic and magnetic forces experienced by the particles, the model also takes into consideration the Brownian motion for small particles and also the shear-induced-diffusion experienced by the plasma borne particles. This diffusion is a result of the random motion generated by the sheared cell-cell collisions in the bloodstream. From the dimensionless version of the advection-diffusion equation for the particle concentration, the motion of the particle in the direction normal to the blood flow is given by the term $(\alpha/\delta)\ (\partial c/\partial y)$, where α is the dimensionless magnetic velocity and δ is the aspect ratio of the vessel. Thus, it was seen that the number of particles that are trapped in the vessel depends on the ratio (α/δ). For the particle diameters considered in the paper, it is found that the shear induced diffusion dominates the Brownian motion. The paper also suggests that shear induced diffusion plays an important role in the deposition of the particles when the diffusive flux is strong enough to balance the advective flux due to the magnetic field. As proved in the paper, in a two-dimensional magnetic field, if the magnetic field is applied externally to the body then there is no point within the body where the magnitude of the force on the particle attains a maximum. This result is important since increasing the magnetic force allows for better trapping of particles, so we would like to maximise magnetic force at the target site. However, the result mentioned above shows that this is possible only if the target region is on the surface of the body.

3 Magnetic particles in a magnetic field

The SPIO particles considered are approximately $120 - 180$nm in diameter [17] and each particle has on the order of three magnetite (iron oxide) cores bound together with a polymer casing. Following [8] the force on a single paramagnetic core is given by

$$\mathbf{F}_{\text{mag}} = (\mathbf{m} \cdot \nabla)\mathbf{B}, \tag{1}$$

where $\mathbf{B}$ is the magnetic field and $\mathbf{m}$ is the magnetic moment of the particle, which in the case of paramagnetic particles depends on the field. For sufficiently weak magnetic fields the force felt by a core is approximated as

$$\mathbf{F}_{\text{mag}} = \frac{m_{\text{sat}}^2}{6kT}\nabla(|\mathbf{B}|^2), \tag{2}$$

where m_{sat} is the saturation magnetisation of the core, k is Boltzman's constant and T is the temperature in Kelvin. The saturation magnetisation can be calculated from the mass saturation magnetisation of magnetite (M_{sat}) according to

$$m_{\text{sat}} = \rho M_{\text{sat}} \frac{4\pi r_{\text{core}}^3}{3}, \tag{3}$$

where ρ is the density of magnetite and r_{core} is the core radius.

Now we proceed to consider a representative field strength. We follow [24] and consider a two-dimensional approximation to a disc magnet next to tissue as depicted in Figure 1. The field can be thought of as generated by two infinitely long wires, each running normal to the page, one carrying charge into the page and one carrying charge out. If the origin to our co-ordinate system lies on the surface of the patient's tissue and we position a magnet with thickness $2d$ and length $2L$ with it's centre at $(0, -d)$ then the field strength is approximately

$$\mathbf{B} = B_0 \nabla \left[\arctan\left(\frac{y+d}{x-L}\right) - \arctan\left(\frac{y+d}{x+L}\right) \right], \tag{4}$$

with some constant B_0 depending on the strength of the magnet.

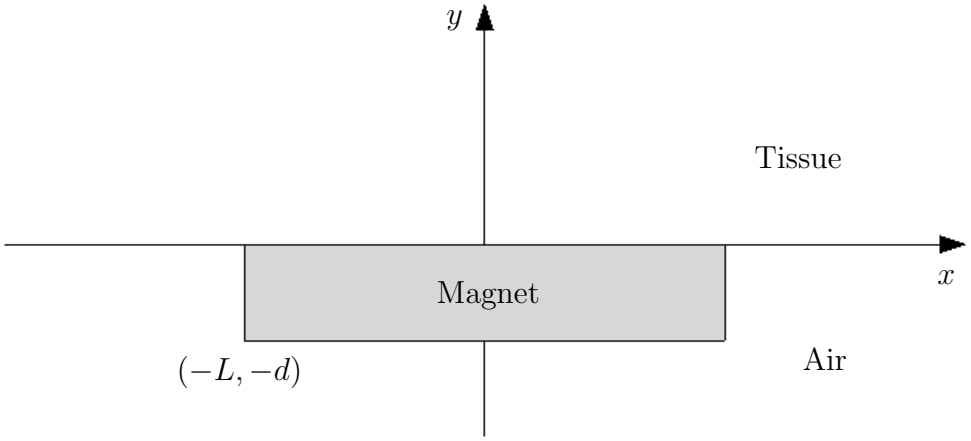

Figure 1: Diagram of magnet against patient's skin, showing co-ordinate system. Magnet has length $2L$, depth $2d$ and is centred at $(0, -d)$.

Parameter	Value	Units	Source
ρ	5.1×10^3	kgm^{-3}	[8]
M_{sat}	50	$\text{Am}^2\text{kg}^{-1}$	[8]
r_{core}	5×10^{-9}	m	$*$
k	1.38×10^{-23}	$\text{m}^2\text{kgs}^{-2}\text{K}^{-1}$	[1]
T	310	K	[2]
d	2×10^{-3}	m	$*$
L	3.5×10^{-3}	m	$*$

Table 1: Parameter values for magnetic force calculation. *Values provided by exerimentalists.

The first observation is to note that the magnetic field can be constructed from dipoles (as opposed to monopoles) so the leading order term in the magnetic field $\mathbf{B}$ scales like $1/r^3$ where r is the distance to the dipole. Therefore we see from (1) that the strength of

the force felt by a core decays roughly like $1/r^7$ with r the distance to the magnet. We calculate the strength of the force generated by our example magnetic set-up using the values in Table 1. We know that the magnet used by the problem presenters generates a field of strength 310mT at the surface of the magnet, so we calculate (4) numerically and pick B_0 so that the average field strength $|\mathbf{B}|$ along the top of the magnet is 310mT.

Figures 2 and 3 show the spatial variation of the magnitude and direction of the force due to the magnet felt by a single core. The key things to note are that the force is always directed towards the magnet and the that the magnitude of the force decays rapidly away from the magnet.

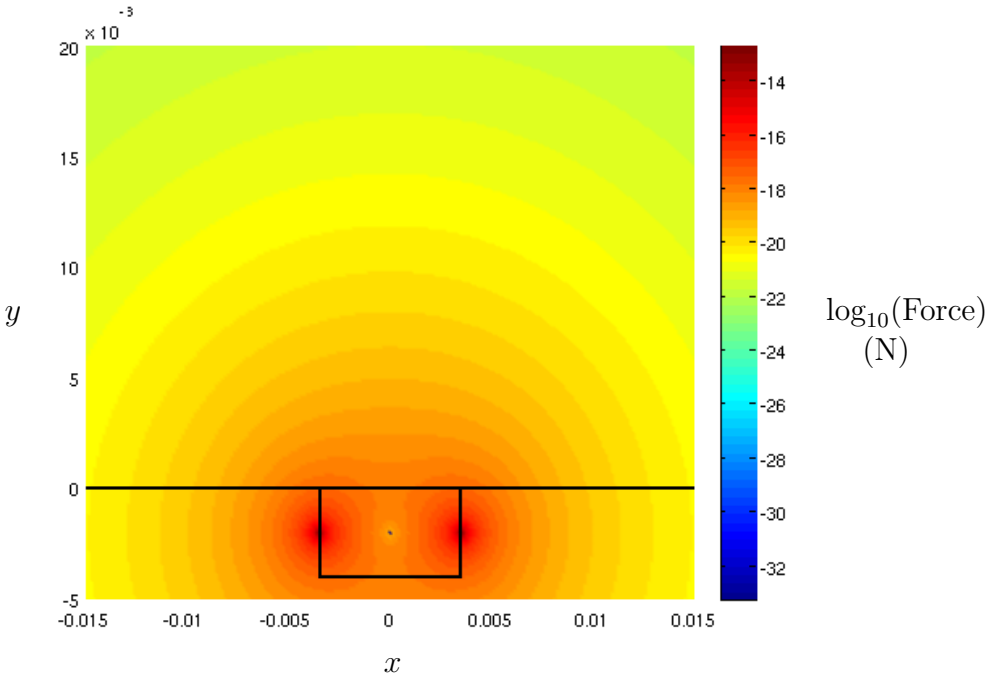

Figure 2: Graph showing the magnitude of force due to the magnet felt by a single core in Newtons. Distances in metres. Skin and magnet outlines are overlaid.

3.1 Force on cell due to magnetic field

A typical amount of iron in a cell that has taken up the type of SPIOs our experimentalists are interested in is 14pg [25]. Given we know the typical size of an iron core within a SPIO and assuming the weight in an iron core is due to the iron, we can approximate the number of cores in a cell as on the order of 10^6. We assume that the cores do not interact with each other, that the polymer coating that holds cores together prevents core interaction. However, it is possible that this assumption would need to be reconsidered if particles arrange and align themselves within cells. Our assumption allows us to sum the forces felt by the cores and approximate the magnetic force on the cell as the force felt by a core at the cell centre multipled by the number cores in the cell. We plot the strength of this force for a section taken along $x = 0$ and show how it decays with distance into the patient in Figure 4.

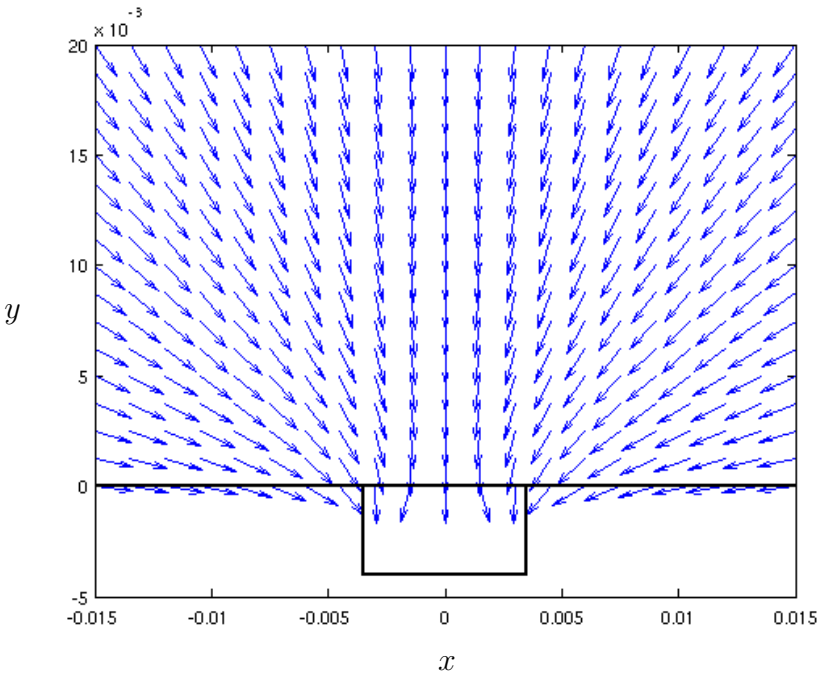

Figure 3: Graph showing the direction of force due to the magnet felt by a single core. Distances in metres. Skin and magnet outlines are overlaid.

4 Effect of magnet on cells in bloodstream

Blood vessels are made up of capillaries, arteries and arterioles, veins and venules all having varied radius. The network formed by the blood vessels is thus quite complex, tubular and extensive. Also, blood comprises of various constituents including red blood cells, white blood cells, platelets, plasma and its solutes. A cell, loaded with superparamagnetic particles, moving in the bloodstream experiences drag due to the blood flow. The particles within the cell experience a force due to the externally applied magnetic field.

Here, we consider three cases where, under certain assumptions, we can calculate the drag on the cell. We consider if it would be possible to trap the cell at the site of tissue injury by balancing the drag and the force generated by the magnetic field.

4.1 Large vessel, cell far from vessel wall

In this case, let us assume that the cell is a small spherical particle of with approximate radius $a = 10\ \mu$m, [10]. The radius is very small compared to the width of the artery. The drag on the cell can then be approximated by Stoke's law and is given as

$$F_s = 6\pi\mu a\,(V - u)$$

where, $\mu = 10^{-3}$kg m^{-1} s^{-1} [24] is the viscosity of the blood in the artery, V is the velocity of the cell and $u = 1 \times 10^{-1}$ m s^{-1} [8] is the velocity of blood. Since we want the cell to remain stationary at the site of injury, we consider $V = 0$. Thus we have,

$$F_s = 6\pi\mu a\, u \approx 10^{-8}\ \text{N}$$

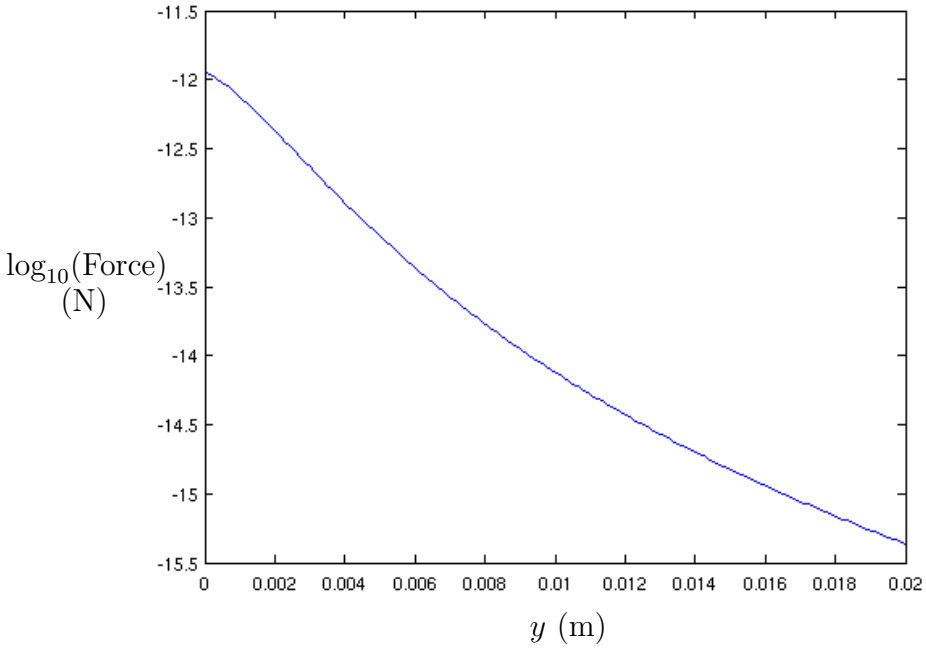

Figure 4: Graph magnitude of magnetic force felt by a cell as a function of distnce away from the magnet along $x = 0$.

4.2 Large vessel, cell near to vessel wall

As the cell moves with the bloodstream, it may happen that under the influence of magnetic field, the cell eventually comes very close to the vessel wall. In this case, the Stoke's law assumptions break down. However, the drag can then be approximated as

$$F_s \;=\; 6\pi\mu a^2 K_f \left.\frac{\partial U}{\partial n}\right|_{wall} \;\approx\; 6\times 10^{-9}\ \mathrm{N}$$

where $K_f \;=\; 1.858$ [24] and $\partial U/\partial n$ is evaluated at the nearest point on the wall. The equation is adopted from [24]. A typical arteriole shear rate $\partial U/\partial n = 6\times 10^2$ taken from [8] is used in this approximation.

4.3 Small vessel

Next, we consider smaller vessels, like capillaries, with diameter comparable to that of the cell. In this case, on entering the vessel, the cell would obstruct the flow of blood through the vessel thus creating a pressure drop inside the vessel. We thus calculate the drag on the cell as the force generated due to the pressure drop. The force is then given as

$$F_s \;=\; \pi a^2 (P_1 - P_2) \;\approx\; 10^{-7}\ \mathrm{N}$$

where $P_1 \;= 32$ mmHg, $P_2 \;=\; 15$ mmHg are the values of the pressure at either sides of the cell [14].

By comparing the force due to the flow with the magnetic forces calculated in the previous section we can see that the magnet is unlikely to be able to produce a sufficiently strong force to tether a cell in the bloodstream.

5 Numerical simulations

In this section we present some numerical solutions for a simple model of a cell in a blood vessel in the presence of a magnetic field. The position and deformation of the cell not only depends on the interaction between the flow and the cell, which are quite complex in such a geometry, but also on the initial position of the cell(s). In the simulations, we consider the two-dimensional problem. Our problem is a simple fluid/structure interaction and can be modelled by Navier–Stokes equations for the fluid flow and Newton–Euler equations for the cell. These two problems can be coupled in a simple manner:

(i) The action of fluid on the cell is modelled by the hydrodynamic force and torque acting on its surface. They are used as the right-hand sides of Newton–Euler equations.

(ii) The action of the cell on fluid can be modelled by no-slip boundary conditions on the cell (in the Navier–Stokes equations).

However, this explicit coupling can be numerically unstable and its resolution often requires very small time steps. In addition, as we have chosen to use the finite element method (FEM) (for accuracy) and since the position of the cell evolves in time, we would have to remesh the computational domain at each time step or at least every few time steps.

5.1 Description of the numerical scheme

5.1.1 Bi-Phasic Model (Fluid-Bubble)

The difficulties discussed above prompt us to choose another strategy to model our problem. Instead of using Newton–Euler equations for modelling the cell motion and Navier–Stokes equations for the fluid flow, we use a bi-phasic model assuming that the cell and the blood can be treated as two Newtonian fluids with different densities and viscosities. This is equivalent to describing the cell as an incompressible bubble surrounded by a fluid. We consider the Navier–Stokes equations using the level set method, see [7]. We write

$$\rho(\phi(x,t))\partial_t u + \rho(\phi(x,t))(u.\nabla u) - \mu(\phi(x,t))\Delta u + \nabla p = f \ , \tag{5}$$

where

$$\rho(x,t) = \begin{cases} \rho_f & \forall x \in \Omega_f, \\ \rho_b & \forall x \in \Omega_b, \end{cases} \quad \text{and} \quad \mu(x,t) = \begin{cases} \mu_f & \forall x \in \Omega_f, \\ \mu_b & \forall x \in \Omega_b, \end{cases} \tag{6}$$

and Ω_f is the fluid or blood region and Ω_b is the cell or bubble region. We write

$$\rho(\phi) = \rho_b + (\rho_f - \rho_b)H(\phi) \quad \text{and} \quad \mu(\phi) = \mu_b + (\mu_f - \mu_b)H(\phi), \tag{7}$$

where $H(\phi)$ is the Heaviside function and $\phi(x,t)$ is the level set function defined as

$$\begin{cases} \phi(x,t) > 0 & \forall x \in \Omega_f \\ \phi(x,t) < 0 & \forall x \in \Omega_b \\ \phi(x,t) = 0 & \forall x \in \Gamma \end{cases} \tag{8}$$

The evolution of the interface Γ at each time t is described by the advection of the level set function $\phi(x,t)$; this is to say that $\phi(x,t)$ satisfies the following problem:

$$\begin{cases} \partial_t \phi + u\ \nabla \phi = 0 & \forall x \in \Omega \times (0,T) \\ \phi = \phi_{in} & on\ \ \Sigma_{in} \\ \phi = \phi_0 & \forall x \in \Omega\ at\ t = 0 \end{cases} \tag{9}$$

$\Sigma_{in} = \{(x,t) \in \partial\Omega \times (0,T); u.n < 0\ \}$ and u is the velocity field. The initial position of the cell is set by ϕ_0. It has to be noted that for our simulations, we use

(i) A relaxation parameter λ $(0 \leq \lambda \leq 1)$ so that we can balance the effect of the magnet to the fluid on the bubble, i.e. we write $u = \lambda u_f + (1-\lambda)u_b$.

(ii) The heaviside function is replaced with

$$H(\phi) = \begin{cases} 0 & if \quad \frac{\phi}{|\nabla\phi|} < -\varepsilon \\ \frac{1}{2}(1 + \frac{1}{\varepsilon}\frac{\phi}{|\nabla\phi|} + \frac{1}{\pi}\sin(\frac{\pi}{\varepsilon}\frac{\phi}{|\nabla\phi|})) & if \quad -\varepsilon \leq \frac{\phi}{|\nabla\phi|} \leq \varepsilon \\ 1 & if \quad \frac{\phi}{|\nabla\phi|} > \varepsilon \end{cases} \tag{10}$$

to be able to project it on our mesh. The interval $[-\varepsilon, \varepsilon]$ is the thickness of the interface between the fluid and the cell. Note that the heaviside function $H(\phi)$ does not depend on ϕ but on $\frac{\phi}{|\nabla\phi|}$. Effectively, after few iterations, certain level lines get closer or far away from each other varying the thickness of the membrane. To overcome this problem, we use $\frac{\phi}{|\nabla\phi|}$ as an approximation of the distance function in the neighbourhood of the interface.

5.1.2 Algorithm

- Update $\rho(\phi)$ and $\mu(\phi)$
- Solve the Navier Stokes equation with f (Magnetic Field force)
- Use the velocity of Navier Stokes Equation to advect ϕ.

5.2 Results

The numerical experiments are done using FreeFem++ [9]. The results obtained are as follows:

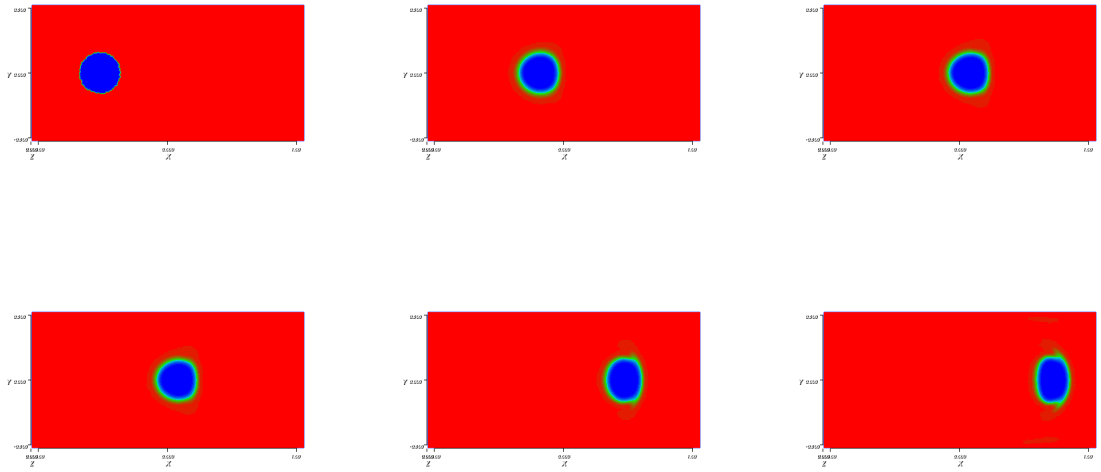

Figure 5: Numerical results without magnet (only fluid effects).

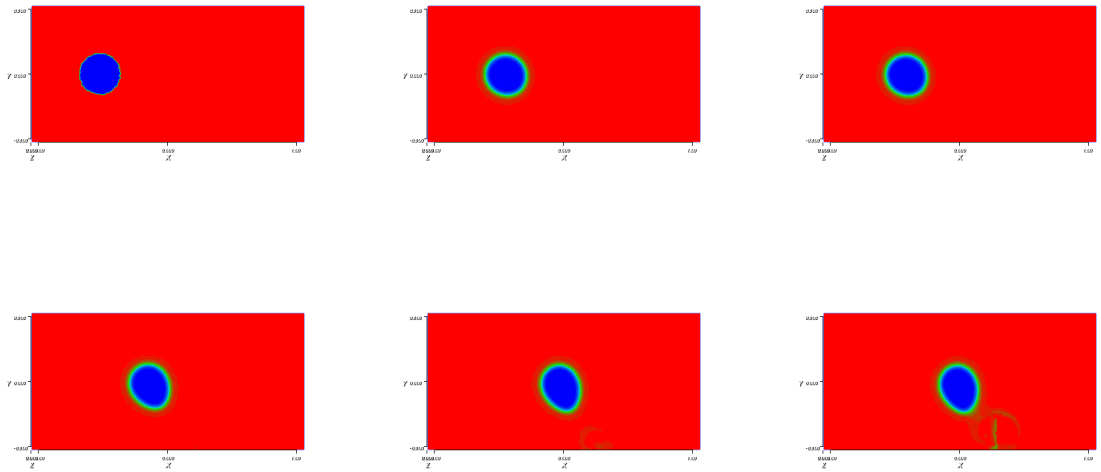

Figure 6: Low influence of the magnet ($\lambda = 0.85$).

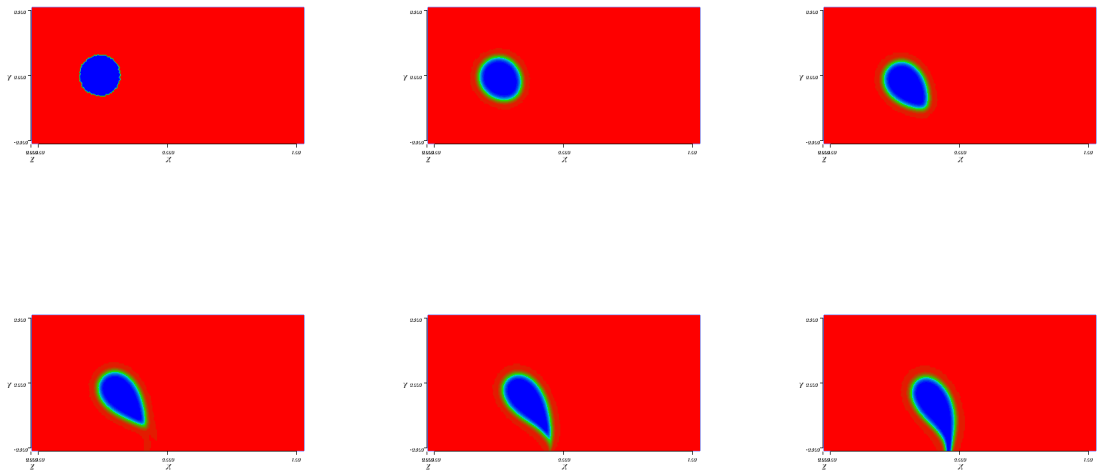

Figure 7: High influence of the magnet ($\lambda = 0.35$).

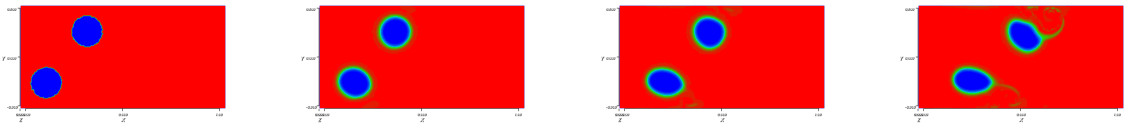

Figure 8: Two cells and low magnet ($\lambda = 0.85$). In this last numerical experiment we noticed numerically unstable behaviour.

6 Conclusions

The previous work on directing paramagnetic particles in the bloodstream with magnets discussed above proves that in two-dimensions the magnetic force felt by the particles cannot attain a maximum away from the surface of the magnet. We attempted, but were unable to extend this result to three dimensions during the study group. However, it seems safe to conclude that any static arrangement of magnets on a patient's skin, capable of focussing magnet force at a target site deep in the tissue would have to be truly three-dimensional, if it exists at all.

We demonstrated through example calculations that the force felt by magnetic particles decays rapidly, like $1/r^7$, away from the magnet. This result will enable the experimentalists to approximate how strong a force their magnet will generate at a given distance into tissue. Whilst the forces due to the magnet and the blood differ in magnitude making it unlikely that the magnet will be strong enough to fix the position of an SPIO loaded cell in the bloodstream, they could slow cells down or cause their paths through the vessel to deviate sufficiently to substantially increase the likelihood of the cell coming into contact with the cell wall. We shall expand on this statement in the next section.

The numerical results of §5.1 demonstrate a possible framework for numerical simulations of cell motion through the bloodstream in the presence of a magnet. The interface between cell and blood is seen to diffuse at some of the later time points and there is some pinching of the cell under the influence of strong magnets. Both these problems could be addressed in future work by incorporating a model of the cell membrane.

7 Future Directions

7.1 Extravasation

In order to exit the bloodstream, MSCs first roll along the endothelial cells that form the inner surface of the blood vessel. This action appears to slow them down until they are able to adhere to the surface, flatten and then deform to crawl through spaces they create between the endothelial cells. Further work could consider the effect that a magnetic force may have on slowing cells to encourage rolling and slowing rolling to encourage adhesion. Modelling could be useful in determining how strong a magnetic force would need to be to have a sufficient effect on this process. A good starting point would be the model of the probability of extravasation in a magnetic field presented in [21].

7.2 Magnetotaxis

One interesting problem that we did not have time to address in the course of the study group concerns how loading cells with magnetic particles influences their crawling motion. The supplementary material to [21] claims that, because the magnetic force on a cell is so much smaller than the force a cell generates in order to crawl through tissue, the magnetic particles have no effect on cells once they leave the bloodstream. However, [32] demonstrates that magnetic fields not dissimilar in strength to those considered here a considerable effect on the chemotaxis of magnetically labelled *Dicytsostelium* cells. Some

simple experiments, perhaps magnetically labelled cells crawling on a microscope slide in the presence of magnet, coupled with mathematical modelling could help develop understanding and quantification of this behaviour, if it exists for MSCs.

References

[1] Codata internationally recommended values of the fundamental physical constants. http://physics.nist.gov/cuu/Constants/index.html.

[2] Wikipedia. http://en.wikipedia.org/wiki/Human_body_temperature.

[3] C.J. Centeno and S.J. Faulkner. The use of mesenchymal stem cells in orthopedics. *Stem Cells and Cancer Stem Cells, Volume 1*, pages 173–179, 2012.

[4] G. Chamberlain, J. Fox, B. Ashton, and J. Middleton. Concise review: mesenchymal stem cells: their phenotype, differentiation capacity, immunological features, and potential for homing. *Stem cells*, 25(11):2739–2749, 2007.

[5] M. Dominici, K. Le Blanc, I. Mueller, I. Slaper-Cortenbach, FC Marini, DS Krause, RJ Deans, A. Keating, DJ Prockop, and EM Horwitz. Minimal criteria for defining multipotent mesenchymal stromal cells. the international society for cellular therapy position statement. *Cytotherapy*, 8(4):315–317, 2006.

[6] A.J. El Haj et al. An in vitro model of mesenchymal stem cell targeting using magnetic particle labeling. Journal of Tissue Engineering and Regenerative Medicine, 2012.

[7] A. Ern and J.-L. Guermond. *Éléments finis: théorie, applications, mise en oeuvre*, volume 159. Springer Verlag, 2004.

[8] A.D. Grief and G. Richardson. Mathematical modelling of magnetically targeted drug delivery. *Journal of Magnetism and Magnetic Materials*, 293(1):455–463, 2005.

[9] F. Hecht and O. Pironneau. Freefem++. Laboratoire de Jacques Louis Lions, Paris 6.

[10] Z. Huang, N. Pei, Y. Wang, X. Xie, A. Sun, L. Shen, S. Zhang, X. Liu, Y. Zou, J. Qian, et al. Deep magnetic capture of magnetically loaded cells for spatially targeted therapeutics. *Biomaterials*, 31(8):2130–2140, 2010.

[11] A. Ito, M. Shinkai, H. Honda, and T. Kobayashi. Medical application of functionalized magnetic nanoparticles. *Journal of bioscience and bioengineering*, 100(1):1–11, 2005.

[12] S.K. Kang, I.S. Shin, M.S. Ko, J.Y. Jo, and J.C. Ra. Journey of mesenchymal stem cells for homing: Strategies to enhance efficacy and safety of stem cell therapy. *Stem Cells International*, pages 1–11, 2012.

[13] S. Kestendjieva, D. Kyurkchiev, G. Tsvetkova, T. Mehandjiev, A. Dimitrov, A. Nikolov, and S. Kyurkchiev. Characterization of mesenchymal stem cells isolated from the human umbilical cord. *Cell biology international*, 32(7):724–732, 2008.

[14] E.K. Kozlova, A.M. Chernysh, and T.N. Matteys. Modeling of blood flow as the result of filtration-reabsorption processes in capillaries. *Advances in Physiology Education*, 23(1):32–39, 2000.

[15] P.G. Kyrtatos, P. Lehtolainen, M. Junemann-Ramirez, A. Garcia-Prieto, A.N. Price, J.F. Martin, D.G. Gadian, Q.A. Pankhurst, and M.F. Lythgoe. Magnetic tagging increases delivery of circulating progenitors in vascular injury. *JACC: Cardiovascular Interventions*, 2(8):794–802, 2009.

[16] L. LaConte, N. Nitin, and G. Bao. Magnetic nanoparticle probes. *Materials today*, 8(5):32–38, 2005.

[17] M. Laniado and A. Chachuat. The endorem tolerance profile. *Der Radiologe*, 35(11 Suppl 2):S266–70, 1995.

[18] K. Ley, C. Laudanna, M.I. Cybulsky, and S. Nourshargh. Getting to the site of inflammation: the leukocyte adhesion cascade updated. *Nature Reviews Immunology*, 7(9):678–689, 2007.

[19] A.H. Lu, E.L. Salabas, and F. Schüth. Magnetic nanoparticles: synthesis, protection, functionalization, and application. *Angewandte Chemie International Edition*, 46(8):1222–1244, 2007.

[20] C.Ã.Š. Nombela-Arrieta, J. Ritz, and L.E. Silberstein. The elusive nature and function of mesenchymal stem cells. *Nature Reviews Molecular Cell Biology*, 12(2):126–131, 2011.

[21] M.R. Owen, I.J. Stamper, M. Muthana, G.W. Richardson, J. Dobson, C.E. Lewis, and H.M. Byrne. Mathematical modeling predicts synergistic antitumor effects of combining a macrophage-based, hypoxia-targeted gene therapy with chemotherapy. *Cancer research*, 71(8):2826–2837, 2011.

[22] Q.A. Pankhurst, J. Connolly, SK Jones, and J. Dobson. Applications of magnetic nanoparticles in biomedicine. *Journal of physics D: Applied physics*, 36(13):R167–R181, 2003.

[23] D.J. Prockop. Marrow stromal cells as stem cells for nonhematopoietic tissues. *Science*, 276(5309):71–74, 1997.

[24] G. Richardson, L. Cummings, J. King, E. Gaffney, L. Hazelwood, and J. Chapman. Drug delivery by magnetic microspheres. Maths in Medicine Study Group Report, 2000.

[25] J. Riegler, J.A. Wells, P.G. Kyrtatos, A.N. Price, Q.A. Pankhurst, and M.F. Lythgoe. Targeted magnetic delivery and tracking of cells using a magnetic resonance imaging system. *Biomaterials*, 31(20):5366–5371, 2010.

[26] H.J. Rippon and A.E. Bishop. Embryonic stem cells. *Cell proliferation*, 37(1):23–34, 2004.

[27] B. Rüster, S. Göttig, R.J. Ludwig, R. Bistrian, S. Müller, E. Seifried, J. Gille, and R. Henschler. Mesenchymal stem cells display coordinated rolling and adhesion behavior on endothelial cells. *Blood*, 108(12):3938–3944, 2006.

[28] S.A. Scherjon, C. Kleijburg-van der Keur, G.M.J.S. de Groot-Swings, F.H.J. Claas, W.E. Fibbe, H.H.H. Kanhai, et al. Isolation of mesenchymal stem cells of fetal or maternal origin from human placenta. *Stem Cells*, 22(7):1338–1345, 2004.

[29] S.A. Scherjon, C. Kleijburg-van der Keur, W.A. Noort, F.H.J. Claas, R. Willemze, W.E. Fibbe, H.H.H. Kanhai, et al. Amniotic fluid as a novel source of mesenchymal stem cells for therapeutic transplantation. *Blood*, 102(4):1548–1549, 2003.

[30] C. Sun, J.S.H. Lee, and M. Zhang. Magnetic nanoparticles in MR imaging and drug delivery. *Advanced drug delivery reviews*, 60:1252–1265, 2008.

[31] A. Uccelli, L. Moretta, and V. Pistoia. Mesenchymal stem cells in health and disease. *Nature Reviews Immunology*, 8(9):726–736, 2008.

[32] C. Wilhelm, C. Riviere, and N. Biais. Magnetic control of dictyostelium aggregation. *Physical Review E*, 75(4):041906, 2007.

[33] P.A. Zuk, M. Zhu, P. Ashjian, D.A. De Ugarte, J.I. Huang, H. Mizuno, Z.C. Alfonso, J.K. Fraser, P. Benhaim, and M.H. Hedrick. Human adipose tissue is a source of multipotent stem cells. *Molecular biology of the cell*, 13(12):4279–4295, 2002.